Atmospheric dispersion and ground deposition induced by the Fukushima Nuclear Power Plant accident A local-scale simulation and sensitivity study

I. Korsakissok, Anne Mathieu, Damien Didier

Atmospheric Environment 70 (2013) 267–279

Contents lists available at SciVerse ScienceDirect

Atmospheric Environment

journal homepage: www.elsevier.com/locate/atmosenv

Atmospheric dispersion and ground deposition induced by the Fukushima Nuclear Power Plant accident: A local-scale simulation and sensitivity study

I. Korsakissok*, A. Mathieu, D. Didier

Institut de Radioprotection et de Sûreté Nucléaire (IRSN), PRP-CRI, SESUC, BMTA, Fontenay-aux-Roses 92262, France

HIGHLIGHTS

- ► We model atmospheric dispersion of the Fukushima accident at local scale (80 km).
- ► Comparisons to gamma dose rate measurements are within a factor 2–5.
- ► Comparisons to deposition measurements are within a factor 5–10.
- ► Source term is the most sensitive parameter.
- ► Gamma dose rate, especially peak values, are more sensitive than deposition.

ARTICLE INFO

Article history:
Received 15 October 2012
Received in revised form
21 December 2012
Accepted 3 January 2013

Keywords:
Atmospheric dispersion
Radionuclides
Fukushima
Model evaluation
Gamma dose rate
Sensitivity

ABSTRACT

Following the Fukushima Daiichi Nuclear Power Plant (FNPP1) accident on March 2011, radioactive products were released in the atmosphere. Simulations at local scale (within 80 km of FNPP1) were carried out by the Institute of Radiation Protection and Nuclear Safety (IRSN) with the Gaussian Puff model pX, during the crisis and since then, to assess the radiological and environmental consequences. The evolution of atmospheric and ground activity simulated at local scale is presented with a "reference" simulation, whose performance is assessed through comparisons with environmental monitoring data (gamma dose rate and deposition). The results are within a factor of 2–5 of the observations for gamma dose rates (0.52 and 0.85 for FAC2 and FAC5), and 5–10 for deposition (0.31 for FAC2, 0.73 for FAC5 and 0.90 for FAC10). A sensitivity analysis is also made to highlight the most sensitive parameters. A source term comparison is made between IRSN's estimation, and those from Katata et al. (2012) and Stohl et al. (2011). Results are quite sensitive to the source term, but also to wind direction and dispersion parameters. Dry deposition budget is more sensitive than wet deposition. Gamma dose rates are more sensitive than deposition, in particular peak values.

1. Introduction

On March 11th 2011, an earthquake of magnitude 9.0 occurred off northeastern Japan, causing a tsunami and damaging the Fukushima Daiichi Nuclear Power Plant (FNPP1). As a result, radioactive products were released in the atmosphere. During the emergency phase, the Institute of Radiation Protection and Nuclear Safety (IRSN) was asked to provide its expertise in support of the French authorities. Since then, the institute has been working on improving its assessment of the terrestrial and marine contamination (Mathieu et al., 2012; Bailly du Bois et al., 2012). Understanding the formation process of highly contaminated areas cannot be achieved through measurements only. While several kinds of measurements are available, they only yield partial information: gamma dose rates devices have a high temporal resolution, but are integrated overall gamma-emitters, and are too scarce to provide a good spatial coverage. Soil samplings and airborne readings provide maps of the contamination, but no information on short-lived species, noble gases, and temporal variations. Thus, improving atmospheric dispersion simulations remains a key issue, especially for dose assessments.

* Corresponding author. Tel.: +33 1 58 35 85 49; fax: +33 1 46 54 39 89.
E-mail address: irene.korsakissok@irsn.fr (I. Korsakissok).

1352-2310
http://dx.doi.org/10.1016/j.atmosenv.2013.01.002

To this day, most numerical studies have focused on reconstructing the source term using environmental data, either at large scale (Stohl et al., 2011,Winiarek et al., 2012), or at local scale (Katata et al., 2012), and using it for dose assessments (e.g. Morino et al., 2011; Terada et al., 2012). Numerical simulations and model-to-data comparisons at local scale are scarce, partly because of the difficulty to produce satisfactory meteorological fields at that scale. Such studies (Chino et al., 2011 and following papers) use gamma dose rates, but not deposition measurements (except Terada et al., 2012 which is based on prefectural measurements at Japan scale). The existing studies were conducted with a given source term and set of deposition parameters, but no extensive sensitivity study has been carried out.

This paper presents the evolution of atmospheric and ground activity simulated at local scale (within 80 km of FNPP1). Simulations are made with pX, IRSN's Gaussian puff model. The pX model is part of the operational platform C3X, which is used by IRSN's Emergency Response Center in case of an accidental radioactive release. The aim of this study is to better understand the formation processes of the contaminated areas, but also to give new insights on the pertinence and limitations of model evaluation tools and indicators in accidental situations. Indeed, usual Gaussian model evaluations are made on simple, well-known dispersion experiments. The Fukushima accident provides an unprecedented case to evaluate atmospheric dispersion models devoted to radionuclides, with many environmental measurements. We try to highlight advantages and shortcomings of each kind of measurements and of statistical indicators used to evaluate a model's performance.

More than one year later, many uncertainties remain, especially on the source term (release kinetics, source height, and isotopic composition) and meteorology. Besides, uncertainties in simulation parameters such as dry deposition velocities and scavenging coefficients cannot be neglected. Our sensitivity study is aimed at identifying the most sensitive simulation parameters and input data.

This paper is organized as follows: first, input data and simulation set-up are described for a "reference" configuration (Section 2). Then, this reference simulation is compared to gamma dose rate and deposition measurements (Section 3). Finally, the sensitivity simulations are presented and discussed based on total deposition budget and model-to-data comparisons (Section 4).

2. "Reference" simulation set-up and input data

2.1. Meteorological data

2.1.1. Wind

Operational forecasts from the European Center for Medium-Range Weather Forecasts (ECMWF) with a spatial resolution of $0.125^\circ \times 0.125^\circ$ and a time resolution of 3 h were used. The model does not resolve the complex topography of the Fukushima area, which is located close to the sea and within 10 km of a mountainous area. The dataset was therefore analyzed and compared with available meteorological data at several monitoring stations in the Fukushima prefecture.

Fig. 1 shows the comparison between the wind at FNPP1 forecast by ECMWF model, and observed by a monitoring car. The modeled wind speed is often higher than the observed values, which is consistent with the difference in heights between observations (monitoring car) and simulation (10 m). Besides, the cell containing FNPP1 is partly over the ocean, where wind speeds are globally higher. The wind direction comparison shows a rather good model-to-data agreement except for some events, especially during March 15 in the evening. During this period, observations clearly indicate a north–northwest plume travel direction, whereas the modeled direction is mostly west. Accuracy in the wind direction is an issue of prime importance at that time since it coincides with heavy rainfalls (cf. Section 2.1.2) and large releases. Therefore, the simulations used in this study were carried out using homogeneous wind fields built with observations at FNPP1 during March 15, between 18 h and midnight, with a 10-min frequency. This solution had its own limitations, since the wind observed at Daiichi was used on a larger domain than its representativity scale, and did not take into account vertical wind shear. For the rest of the simulation, three-dimensional ECMWF data were preferred, to account for the heterogeneity of the flow.

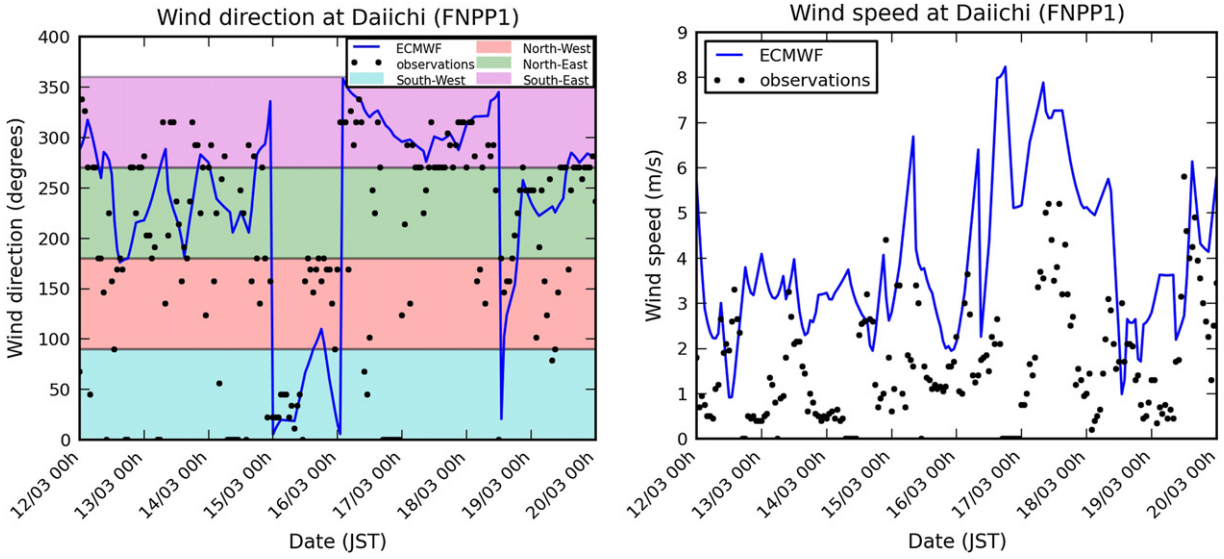

Fig. 1. Comparison of wind observations (1-h median) at FNPP1 and wind given by ECMWF model, between March 12th and 20th. Left: wind direction (the bands of color indicate the plume travel direction), right: wind speed. The ECMWF wind is taken in the cell of FNPP1 (without spatial interpolation), at 10 m. (For interpretation of the references to color in this figure legend, the reader is referred to the web version of this article.)

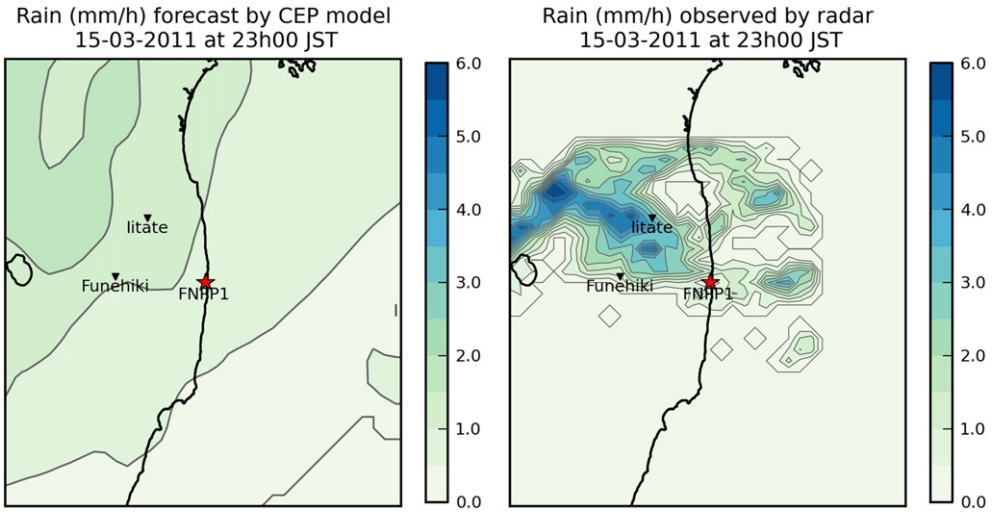

Fig. 2. Maps of rainfall rate on March, 15th at 23 h JST. Left: rain simulated by the meteorological model – Right: radar observations averaged on the same mesh (0.125° resolution).

2.1.2. Rain

During the accident, several rain episodes occurred. The first one took place on 15–16 March and contributed to a significant contamination by wet deposition. The second one happened on 20–23 March, both in the Fukushima region and in Tokyo. The spatial and temporal resolution of the ECMWF model may be insufficient to accurately represent the spatial and temporal variability of rain episodes. On the other hand, rain radar observations provided by the Japan Meteorology Agency[1] have a higher resolution in time and space but may oversee light and localized rainfalls. Both datasets were compared to observed rainfall rates available at several meteorological stations (not shown). Fig. 2 illustrates that radar data improve the spatial resolution of rain, even when averaged on the same grid resolution as modeled data. It also shows the tendency of meteorological forecasts to overestimate the spatial coverage of rainfalls, due to the coarse resolution. Thus, rain radar data are used in the reference simulation.

2.2. Source term

The source term used here reconstructs atmospheric releases occurring between March 12th and 26th, 2011. It includes 73 radioisotopes, based on the French reactor core inventory, corrected to account for the nominal reactor power. The methodology used for this estimation is detailed in other references (Corbin and Denis, 2012; Mathieu et al., 2012; IRSN, 2012).

The main release periods are given in Table 1. Two main release heights were considered. A 20-m height (reactor pressure vessel) is taken whenever pressure decreases happen in the unit, and a 120-m height (exhaust stack) is preferred for specific venting actions. For the hydrogen explosions (events 1 and 3), the source was assumed to be diluted by the heat and momentum of the explosion, within 100 m and 300 m on the vertical respectively (Katata et al., 2012). After March 17th (events 7–10), releases were detected by on-site monitoring devices, but could not be associated to specific units or events. For these releases, simulation results were used to infer the source height. For event 9, a height of 50 m was preferred, which is consistent with the smokes coming from the top of reactor buildings (58 m) at that time.[2]

The radionuclides released in the atmosphere can be classified into (1) noble gases that neither react with other species, nor deposit on the ground, and (2) species that undergo dry and wet deposition. Fig. 3 shows that noble gases were preponderant especially in the first releases (events 1, 2 and 3), since they are more volatile. The total estimated activity released in the atmosphere was 7.18×10^{18} Bq (Becquerel). Noble gases (xenon and krypton) contributed to most of the released activity (91% of the activity), iodine to 6%, and cesium to less than 1%. For the major contributors to gamma dose rate, the estimated released quantity was 1.97×10^{17} Bq for ^{131}I, 1.68×10^{17} Bq for ^{132}I, 1.08×10^{17} Bq for ^{132}Te, 2.06×10^{16} Bq for ^{137}Cs, 2.78×10^{16} Bq for ^{134}Cs and 5.94×10^{18} Bq for ^{133}Xe. The isotopic ratio ^{131}I/^{137}Cs in the source term was initially 12 for Unit 1 and about 9 for Units 2 and 3. These initial values are consistent with the ratio of 10 taken by Chino et al. (2011), based on concentration measurements in rain water and vegetation at local scale.

2.3. Dispersion and deposition parameters

IRSN's Gaussian puff model pX was used for the simulations (Soulhac and Didier, 2008). It handles radioactive decay and decay products with a comprehensive mechanism. Dispersion in the pX model is based on a discrete representation of the atmosphere using Pasquill–Turner stability classes (Turner, 1969). In our simulations, the stability was determined using the temperature gradient between 2 m and 100 m in the meteorological forecasts, for each cell and time step. The Pasquill standard deviation laws (Pasquill, 1961) were used in the reference configuration.

Dry deposition and wet scavenging are crucial processes to model the atmospheric behavior of radionuclides, since the species deposed on the ground still contribute to the gamma dose-rate after the plume departure from the area. The deposition properties of radionuclides strongly depend on three aspects: the gas/aerosols partitioning, the proportion of organic and inorganic forms of iodine, and the aerosol size distribution (Sportisse, 2007).

[1] http://agora.ex.nii.ac.jp/earthquake/201103-eastjapan/weather/data/radar-20110311/.

[2] http://www.tepco.co.jp/en/press/corp-com/release/11032312-e.html.

Table 1
Release periods of the source term, events that caused the releases (when identified), source height and main plume travel direction.

Number	Beginning date	Ending date	Event	Main plume travel direction	Source height
1	12/03 10 h	13/03 09 h	Unit 1 – hydrogen explosion	North, then east	20 m (diluted on 100 m)
2	13/03 08 h	13/03 13 h	Unit 3 – venting	East (Pacific Ocean)	120 m
3	14/03 05 h	14/03 15 h	Unit 3 – venting, then hydrogen explosion	East (Pacific Ocean)	150 m (diluted on 300 m)
4	15/03 00 h	15/03 04 h	Unit 2 - venting	South	120 m
5	15/03 06 h	15/03 21 h	Unit 2 – breach on the wet-well	West, north-west, south	20 m
6	16/03 00 h	16/03 15 h	Units 2 and/or 3 pressure decreases	South	20 m
7	18/03 15 h	18/03 20 h	Unit 3?	North	120 m
8	20/03 15 h	21/03 04 h	Units 2 and/or 3?	South	120 m
9	21/03 15 h	23/03 00 h	Units 2 and 3 (white and gray smokes)	South-west	50 m
10	25/03 08 h	25/03 10 h	Unit 2?	West	120 m

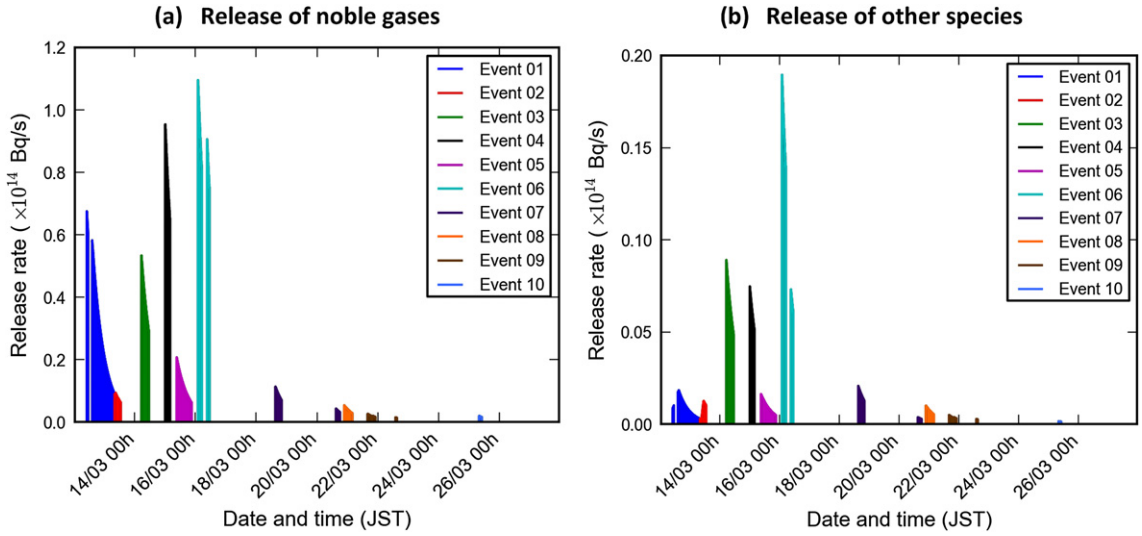

Fig. 3. Time evolution of atmospheric release rate from Fukushima Daiichi Nuclear Power Plant between 12 and 26 March, 2011, for (a) Noble gas and (b) Other species (cesium, iodine, tellurium…).

Without knowledge of these features, simple models were chosen over detailed microphysical modeling. An apparent deposition velocity of 0.2 cm s^{-1} is taken for all particles, notably ^{137}Cs (Brandt et al., 2002). For iodine, 2/3 of released iodine quantity is assumed to be gaseous (molecular) and 1/3 in particulate form. The deposition velocity of molecular iodine I_2 is higher than for particulate matter: 0.7 cm s^{-1} (Baklanov and Sørensen, 2001). The deposition velocities used over sea water are lower than over lands, namely 0.05 cm s^{-1} (Pryor et al., 1999). The scavenging coefficient is given by $\Lambda s = \Lambda_0 \times p_0^B$, with p_0 the rain intensity in mm h^{-1}. In the reference simulation, $\Lambda_0 = 5 \times 10^{-5}$ h mm^{-1} s^{-1} (as in Terada et al., 2012) and $B = 1$.

3. Reference results and discussion

In this section, simulations with the pX model and the reference configuration are analyzed and compared with observations. Statistical indicators used for model-to-data comparisons are defined in Appendix.

3.1. Gamma dose rates

The observations used in this section come from prefectural monitoring devices,[3] along with the data provided by TEPCO (Tokyo Electric Power Company) at Fukushima Nuclear Power Plant 2, hereafter called Daini.[4] Stations with a low-quality signal (too much missing data) were discarded. In total, eight monitoring stations were used (Table 2 and Fig. 7). To compute the simulated gamma dose rates, 135 radionuclides (including 73 emitted species plus their decay products) are taken into account. Dose coefficients (Eckerman and Ryman, 1993) are used to infer dose rates from each species' volume and surface activities. Since the Gaussian model gives an analytical formula of the concentration, the dose rates were directly computed at the stations' locations and no simulation grid was used.

3.1.1. Overall performance on stations

The overall model performance on stations is satisfactory: 52% of data are within a factor of 2 of the observations (FAC2), and 85% are within a factor of 5 (FAC5). The fractional bias is 0.44 which indicates a trend to overestimation, the correlation is 0.72, and the figure of merit in time (FMT) is 0.43. This compares well to typical Gaussian models performance on dispersion experiments (Korsakissok and Mallet, 2009), even though uncertainties on input data are much higher.

The ambient gamma dose rate measured in air comes from two contributions: the direct plume contribution (hereafter called "plume-shine") and the gamma-ray emitted by radionuclides

[3] http://www.pref.fukushima.jp/j/7houbu0311-0331.pdf and http://www.pref.fukushima.jp/j/20-50km0315-0331.pdf.

[4] http://www.tepco.co.jp/en/nu/fukushima-np/f2/data/2011/index-e.html.

Table 2
Comparison of observed and simulated ambient air dose rate at the eight stations: peak time and value (the peak is the maximum value on the whole period of observations), Fac2 and Fac5 (proportion of simulation values within a factor of 2 resp. 5 of the observations). Statistics are made on the whole period (12/03–26/03).

Station name	Event(s) associated with peaks	Observed arrival time (1st peak)	Simulated arrival time (1st peak)	Observed peak value (μGy h^{-1})	Simulated peak value (μGy h^{-1})	Fac2 (%)	Fac5 (%)	FMT
Kawauchi	Event 5; event 9	15/03 11:00	15/03 12:00	11.5	15.7	69	99	0.64
Tamura City	Event 5 (2 peaks)	–	15/03 16:00	–	6.2	5	82	0.19
Funehiki			16/03 06:00		9.4			
Koriyama	Event 5; event 9	15/03 14:00	15/03 17:00	6	3.0	52	99	0.47
Iitate	Event 5	15/03 15:00	15/03 21:00	39.5	57.6	67	97	0.54
Fukushima	Event 5	15/03 16:00	15/03 22:00	24	19.1	92	98	0.79
Minamisoma	Event 1; event 7	12/03 20:00	12/03 19:00	20.0	87	95	100	0.68
Daini (FNPP2)	Event 4; event 6	15/03 00:00	15/03 01:00	94	515	12	88	0.38
Iwaki	Event 4; event 6	15/03 01:00	15/03 03:00	23.7	147	9	16	0.12

deposed on the ground ("ground-shine"). The plume-shine usually is responsible for peak values (high but during a short time), whereas the ground-shine corresponds to the gamma dose-rate measured after the plume departure. Hence, the most numerous gamma-dose rate observations correspond to ground-shine, which decreases slowly due to radioactive decay. The decrease rate of this residual gamma dose rate depends on the radioisotopes deposed on the ground, and on their respective half-life times. Therefore, "classical" indicators such as FAC2 and FAC5 mainly depend on the simulation's ability to forecast deposition, isotopic composition and subsequent decay. In case of an accidental release of radionuclides, an operational simulation should be able to forecast peak values, since they represent an important part of human exposure (through direct radiation and inhalation), and plume arrival times (i.e. the first date when the gamma dose rate value is higher than background value). In the following, we will focus on (1) bias on peak values, (2) plume arrival times and (3) FAC2, FAC5 and FMT. Comparisons are made on hourly-averaged values.

Table 2 gives an overview of the model's performance for each station. Peak values are within less than a factor of two, except for Iwaki, Daini and Minamisoma, where it is overestimated by a factor of five. These three stations are located close to the coast, where the meteorological model often has difficulties forecasting the wind field. Besides, for the two events responsible for the peaks (event 1 for Minamisoma and event 4 for Daini and Iwaki), the meteorological conditions were very stable. Thus, the plume was very thin, and uncertainties in the wind field, station location, and/or release height would have a large impact on the result. At Minamisoma and Iwaki, gamma dose-rate measurements are only available every hour during the main releases periods (prior to March 16). Simulations show a high temporal variability, especially during the plume passage, indicating that the temporal frequency of observations may not be sufficient. The temporal resolution of the wind field (3 h) is also too coarse to account for the wind variability.

On the other stations, the peak values are very well reproduced, although a delay of 6 h in the plume arrival time is observed on the northwestern stations Iitate and Fukushima. At Funehiki, there were no observations at the simulated peak times, and the air dose-rate due to deposition is overestimated by more than a factor of five. For all other stations except Iwaki, more than 80% of simulated values are within a factor 5 of the observations, and the FAC2 is also very good, especially at the northwestern stations. Fig. 4 shows the model-to-data comparisons of gamma dose rate values, for the eight monitoring stations, hour-by-hour. A few singular values are underestimated, especially at Iitate and Fukushima, due to the delay in the plume arrival time.

3.1.2. *Temporal analysis on stations*

Fig. 5 shows the temporal evolution on four of these stations: two are representative of a high contamination level due to wet deposition (Iitate and Fukushima), and two stations where little wet deposition occurs (Minamisoma and Kawauchi). The latter show a time series with several peaks corresponding to plumes coming through the station, and little deposition, while the former show a high contamination by deposition, with a decrease rate over time essentially due to radioactive decay of the deposed isotopes.

At Minamisoma and Kawauchi (Fig. 5(a) and (b)), most peaks are simulated, with a small delay and some overestimation at Kawauchi. Missing peaks are probably due to inaccuracies in the source term, but are small compared to the initial contamination. These two stations illustrate the difficulty to correctly represent both peak values and deposition: at Minamisoma, the peak value is overestimated but the deposition is correctly forecast, while at Kawauchi, the peak value is much better reproduced but the deposition is overestimated after March 22nd. At Iitate and Fukushima, the dose rates are well reproduced, except for the initial delay in the plume arrival (6 h). This delay is also found by other simulations (Katata et al., 2012). Fig. 6 illustrates the contamination processes at two typical

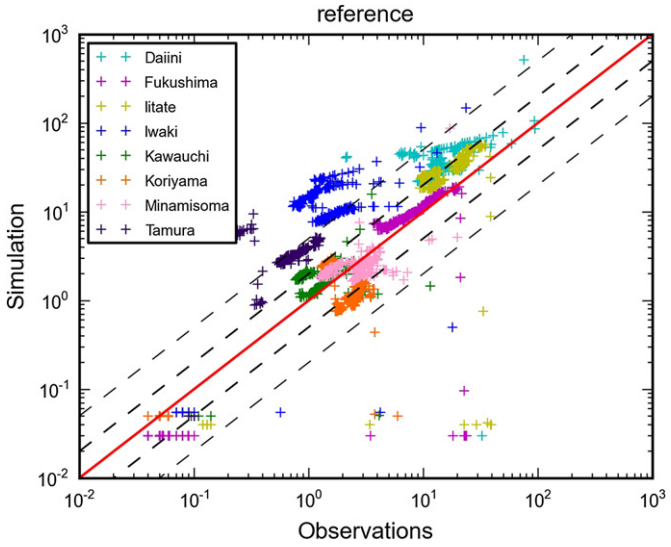

Fig. 4. Scatter plot of gamma dose rate values (μGy h^{-1}) at the eight monitoring stations for the reference simulation. Red line: perfect agreement. Dashed line (bold): factor 2. Dashed line: factor 5.

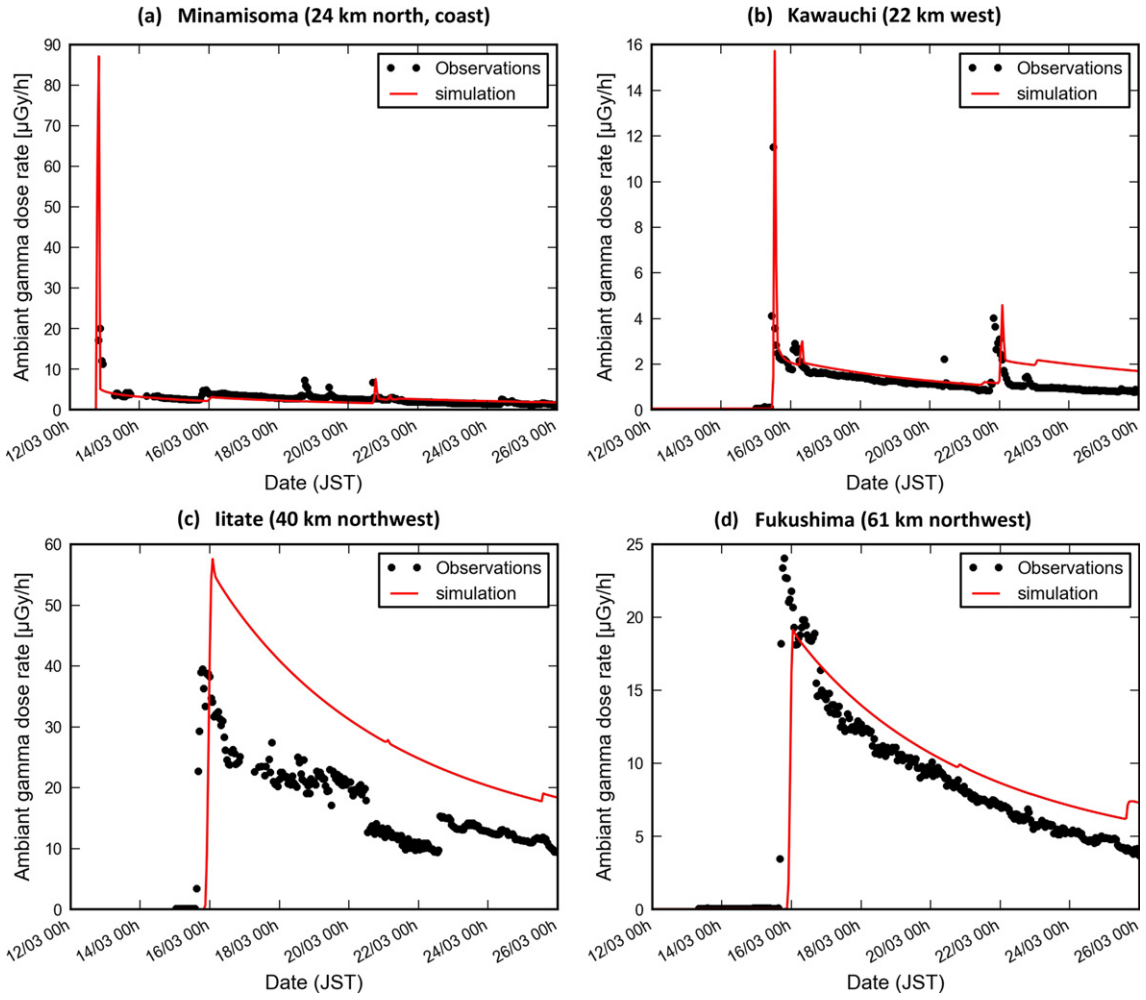

Fig. 5. Comparison of observed and simulated gamma air dose rate at four of the eight monitoring stations. Simulations are made with pX, for the reference configuration.

stations: (a) Kawauchi, where the plume contribution is preponderant (91% of the peak gamma dose rate) and ground shine is only due to dry deposition, and (b) Fukushima, where the wet deposition contribution to the gamma air dose rate is predominant (95% of the peak dose rate). Fig. 6(b) shows that the delay at Fukushima is not due to inaccuracies in the rain timing, but to a delay in the plume arrival time. Indeed, the plume contribution does not increase significantly before 22 h on March 15th. This might be due to uncertainties in the wind field and/or source height.

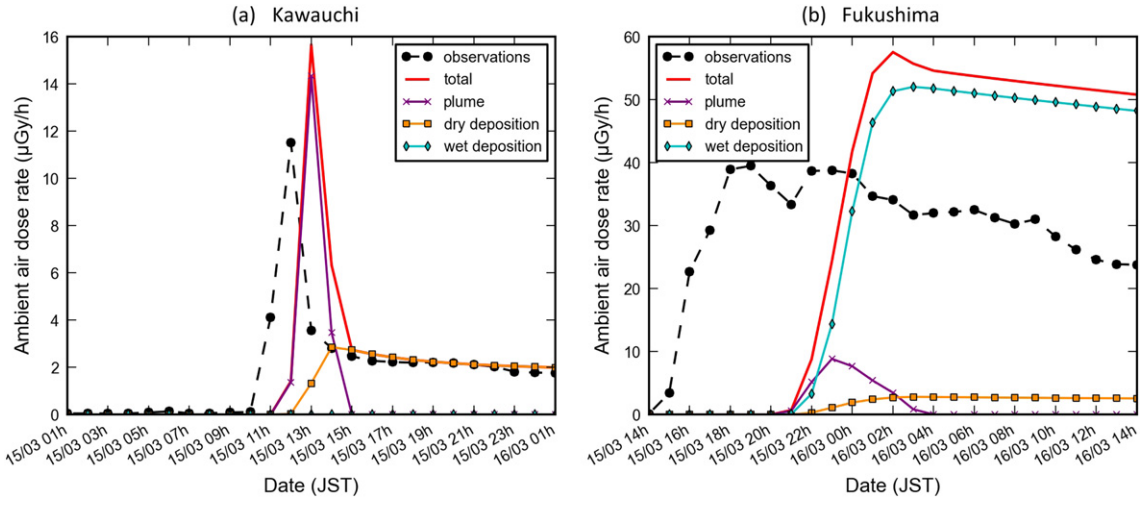

Fig. 6. Plume, dry deposition and wet deposition contributions to the simulated ambient air gamma dose rate at (a) Kawauchi and (b) Iitate.

3.2. Deposition

The simulations used in this section are made on a polar mesh, with circles at 2.5, 5, 10, 15, 20, 25, 30, 40, 50, 65 and 80 km from FNPP1, and a ten-degree step for the angle.

3.2.1. Spatial analysis

Fig. 7 shows the simulated spatial distribution of deposition after the end of releases (March 30, 2011). Dry deposition mostly occurred along the coast, north and south from FNPP1 ((Fig. 7(a)), whereas wet deposition strongly contaminated a northwestern area, including Iitate and Fukushima (Fig. 7(b)). Analyses by event showed that the dry deposition north of FNPP1 was formed during two distinct events: event 1 (12/03) and event 7 (18/03). The southern deposition along the coast corresponds to event 4 (15/03 at 00 h) and event 6 (16/03). Wet deposition mainly corresponds to event 5 (67% of total land deposition occurred within few hours on March 15th), but also occurred on 21/03 and 22/03 (16% of total deposition), south and south-west of the plant (event 9). The dry deposition over the sea is much lower, due to the use of lower deposition velocities over water. The contribution of dry deposition to total deposition is shown Fig. 7(c). It confirms that the northwestern contamination is mainly due to wet deposition (more than 90% of the total deposition), whereas dry deposition contributes to almost 100% deposition along the coast.

Dry and wet deposition patterns are similar for other species than ^{137}Cs, although dry deposition is stronger for molecular iodine. This leads to a higher ratio ^{131}I/^{137}Cs where dry deposition is predominant, especially south of FNPP1 (Fig. 7(d)). This pattern is consistent with observations (Kinoshita et al., 2011). This ratio tends to decrease over time, since the half-life of ^{131}I (eight days) is much lower than for ^{137}Cs (thirty years).

3.2.2. Deposition budget

As Morino et al. (2011) did on Japan scale, we computed the total budget of ^{137}Cs and ^{131}I deposed on the simulation domain through dry and wet deposition (decay-corrected). Their source term comes from Chino et al. (2011), which includes 13 PBq of ^{137}Cs (20.6 PBq in our estimation) and 150 PBq of ^{131}I (197 PBq in our case). Morino et al. (2011) supposed that the gaseous fraction of ^{131}I was 80% of the total release (67% in our case). Their estimation for the Fukushima prefecture can be compared with our land deposition budget within 80 km from FNPP1 (Table 3).

The absolute values are of the same order of magnitude, except for ^{137}Cs dry deposition, where our value is ten times higher. This

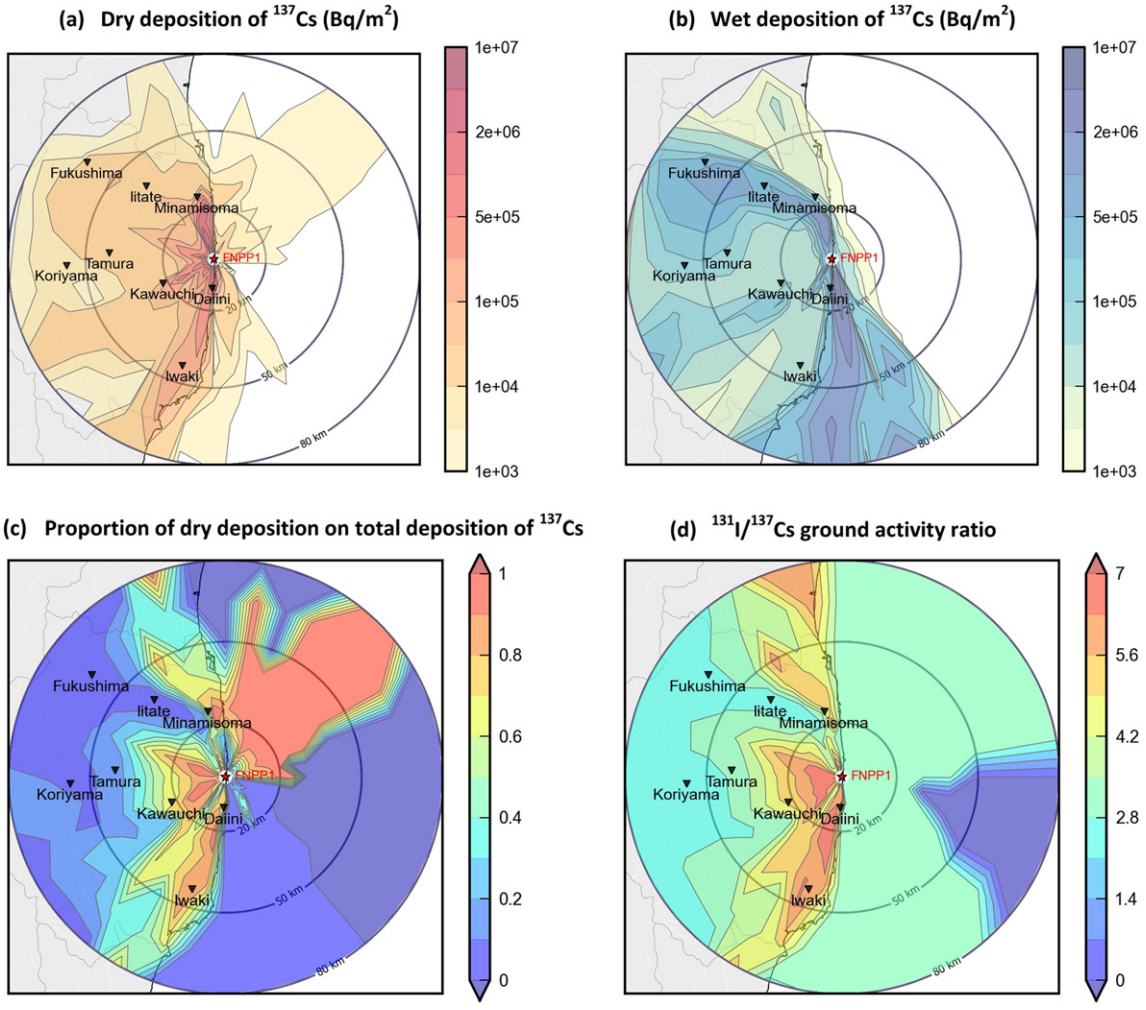

Fig. 7. Spatial distribution of (a) ^{137}Cs dry deposition, (b) ^{137}Cs wet deposition, (c) Ratio of dry deposition on total deposition for ^{137}Cs and (d) ^{131}I/^{137}Cs ground activity ratio. Values are given on March 30, 2011.

Table 3
Simulated ^{137}Cs and ^{131}I loss due to dry and wet deposition: contribution over land and sea, and total on the simulation domain (80 km around FNPP1). (*): deposed quantity normalized by released quantity. Simulations are made with pX, for the reference configuration. Values are given in PBq ($\times 10^{15}$ Bq). The values are decay-corrected for iodine.

		Morino et al., 2011 Fukushima pref. 13,783 km^2	Land 80 km of FNPP1 about 10^4 km^2	Sea 80 km of FNPP1 about 10^4 km^2	Total (land + sea, 80 km radius)
^{131}I (PBq) Decay-corrected	Dry deposition	8.07	7.9	0.3	8.2
	Wet deposition	3.6	6.1	22.0	28.1
	Total deposition	12.3 (8.2%)*	14.0 (7.1%)*	22.3	36.3 (18.4%)*
^{137}Cs (PBq)	Dry deposition	0.047	0.39	0.02	0.39
	Wet deposition	1.48	0.94	2.6	3.9
	Total deposition	1.53 (11.7%)*	1.33 (6.4%)*	2.62	4.29 (20.8%)*

may be due to the lower released amount, and to lower dry deposition velocities (0.1 cm s^{-1} instead of 0.2 cm s^{-1} in our simulations). For gaseous ^{131}I, Morino et al. (2011) took 0.5 cm s^{-1} (0.7 cm s^{-1} in our case). Estimates of total iodine dry deposition are comparable. Wet deposition values are more difficult to compare, without knowledge of the parameterization used. In our case, scavenging is the same for all species. In Morino et al. (2011), the wet deposition scheme seems more efficient for ^{137}Cs, which is in particulate form, than for ^{131}I, which is mostly gaseous. It probably explains the higher proportion of ^{137}Cs deposed over land (12% of their release).

Total deposition values are very close to each other. Compensation between dry and wet deposition partly explains this agreement. Based on airborne monitoring data[5], the total quantity of ^{137}Cs within 80 km of the plant over land was estimated to be about 1.49 PBq, with an uncertainty of ±0.49 PBq (Gonze, M-A, personal communication). Both simulations are within this range.

3.2.3. Comparisons to deposition measurements

Fig. 8 shows the comparison between the simulation and the observations of ^{137}Cs deposition provided by Ministry of Education, Culture, Sports, Science and Technology (MEXT).[6] About 1800 measurements are within our simulation domain. The overall shape of the northwestern contamination (over 10^5 Bq m^{-2}) is correct, but the highest values are located too north compared to the observations. This is probably due to the use of wind observations at FNPP1 at that time, not representative of the wind direction at a larger scale. Thus, the model overestimates deposition north along the coast by more than a factor five (yellow to red points, Fig. 8(c)). The overestimation south, after 40 km, is consistent with gamma dose rates at Iwaki. Fig. 8(d) shows that the agreement is better between 20 and 60 km from the source. Closer to the source, the model tends to overestimate deposition. Between 60 and 80 km, values are underestimated, especially in the northern area (gray and purple points, Fig. 8(c)). In all, 31% of simulated values are within a factor 2 of the observations, 73% within a factor 5, and 90% within a factor 10. The correlation coefficient is 0.34. The figure of merit in space (FMS) depends on the chosen threshold. A high threshold would focus on the model's ability to forecast extreme values. For 10^4 Bq m^{-2} (94% of measurements), the FMS is very good (0.85). For 10^5 Bq m^{-2} (30% of measurements, mainly northwest), it goes down to 0.43, probably because of the misplaced wet deposition zone.

Very close measurement points may differ by a factor 5–10, which may be due to running water or changes in terrain type (school yard, agricultural field…). The simulation gives averaged values, and does not account for local-scale variability. Thus, further analyses of the datasets and aggregating close measurements could improve these comparisons.

4. Sensitivity study

4.1. Sensitivity parameters

Table 4 shows an overview of the parameters chosen for the sensitivity simulations. Simulations were carried out independently for each parameter, to assess their impact on results.

For dispersion, several Gaussian standard deviation formulations were used. For dry and wet deposition, values were taken within the range of the literature, i.e. more or less within a decade (Sportisse, 2007). Mixing the release between 0 and 150 m allowed highlighting the sensitivity to the release height. Several source terms were also compared. The release from Katata et al. (2012) was designed at local scale, including several isotopes to compute the gamma dose rates. Thus, it was included in deposition and gamma dose rate sensitivity runs. The release from Stohl et al. (2011), calibrated on long-range simulations (with a first-guess), did not include short-lived species that are major contributors to gamma dose rate. Thus, it was only used in the comparisons for ^{137}Cs deposition. Another IRSN's estimation, using inverse modeling with gamma dose rate observations (Saunier et al., 2012), was included. Concerning meteorological data, the influence of rain (radar observations versus rain forecasts) and wind fields (with and without wind observations at Daiichi on March 15th) was evaluated.

4.2. Sensitivity results

4.2.1. Sensitivity of total deposition budget of ^{137}Cs

Fig. 9 illustrates the sensitivity of the deposition budget over land. The sensitivity of total deposition is conditioned by that of wet deposition, which accounts for 2/3 of total deposition (cf. Table 3). For total deposition, most simulations are within a factor 2 of the reference simulation, except with the source term from Stohl et al. (2011) which has a higher estimation of ^{137}Cs release (35 PBq of ^{137}Cs). According to airborne observations, the total land deposition within 80 km of FNPP1 should be between 1 and 2 PBq (see Section 3.2.2). Most simulations meet this condition except the *Release_Stohl* and *lmin* configurations. Dry deposition (Fig. 9(a)) is also sensitive to vertical diffusion. Indeed, Briggs urban and constant diffusion parameterizations enhance vertical diffusion, which induces lower dry deposition, since the plume is less concentrated near the ground. Finally, a compensation mechanism between dry and wet deposition appears: lower deposition velocities (*vdmin*) imply that the plume is less depleted near the source. Hence, the plume wash-out by the rain is more efficient, and wet deposition increases (Fig. 9(b)).

[5] http://www.mext.go.jp/english/incident/1304796.htm.
[6] http://www.mext.go.jp/b_menu/shingi/chousa/gijyutu/017/shiryo/__icsFiles/afieldfile/2011/09/02/1310688_1.pdf.

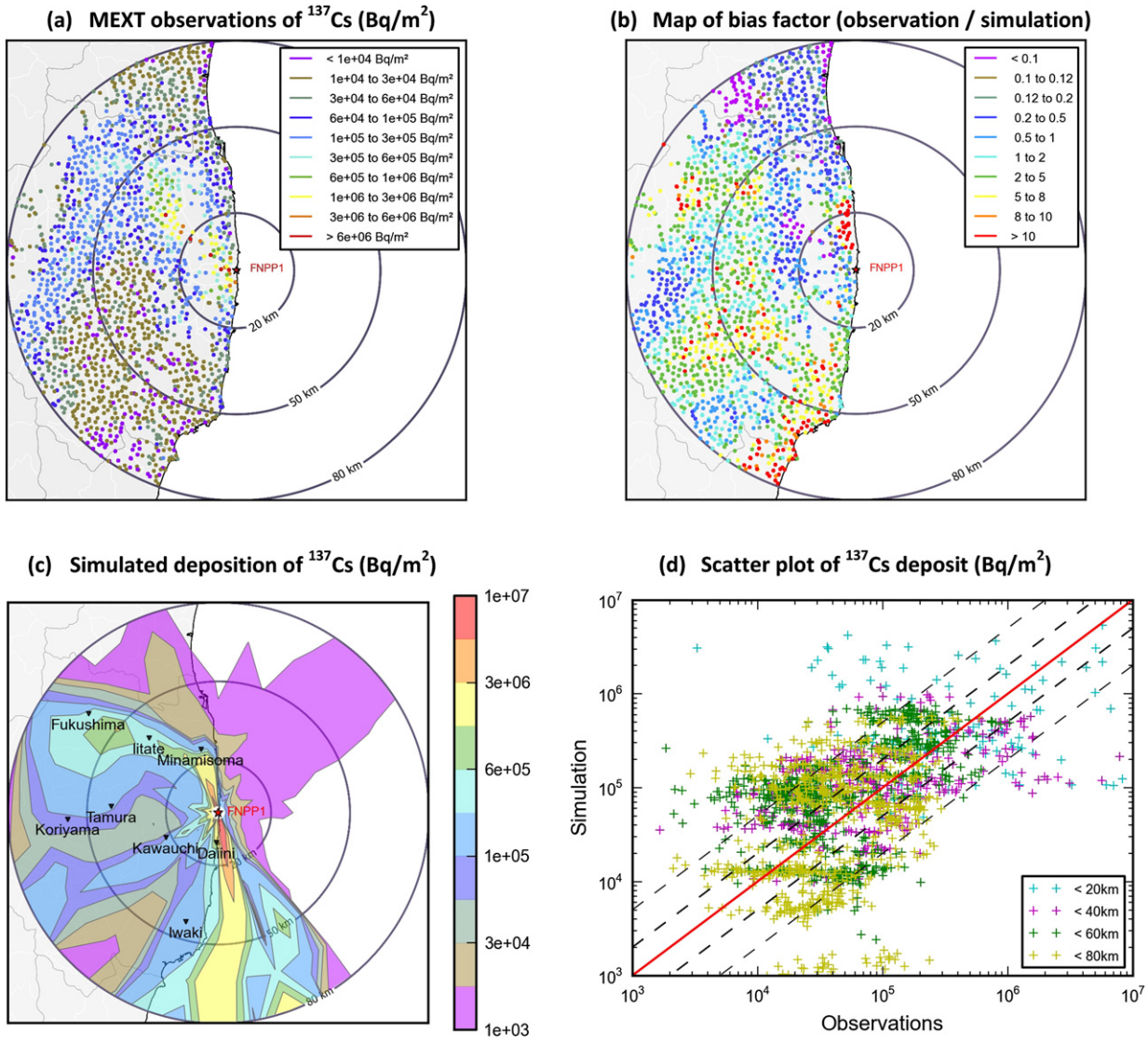

Fig. 8. Comparison of observed and simulated deposition values for ^{137}Cs. (a) Observations from MEXT. (b) Map of bias factor (observation/simulation). (c) Deposition simulated with pX. (d) Scatter plot: Red line: perfect agreement. Dashed line (bold): factor 2. Dashed line: factor 5.

4.2.2. *Sensitivity of spatial deposition of ^{137}Cs*

The sensitivity of spatial deposition may be investigated through statistical indicators used in comparison to MEXT measurements (Fig. 10). They are quite robust to changes in parameterizations such as standard deviations, vertical mixing, and dry deposition. The source term is the most sensitive, along with rain and wind fields. The *Release_Stohl* decreases significantly the FAC2, and changes in meteorological data also reduce the FAC2 (Fig. 10(a)). A low scavenging coefficient (*lmin*) increases FAC2 (0.37), but lowers FAC5 (0.70). FAC2 and FAC5 would not penalize a simulation that would homogenize the deposition. For instance, a "simulated" homogeneous deposition of 10^5 Bq m^{-2}, compared to

Table 4
Sensitivity simulations: overview of all simulation parameters modified in the sensitivity runs. Each parameter is made to vary independently from one another. For each sensitivity parameter, the name used in the figures is given in brackets.

Parameter	Reference	Value 1 (*name*)	Value 2 (*name*)	Value 3 (*name*)
Standard deviations	Pasquill	Briggs rural (*briggs_rural*)	Briggs urban (*briggs_urban*)	Constant diffusion K (*diff*)
Dry deposition particles (iodine)	2×10^{-3} (7×10^{-3}) m s^{-1}	5×10^{-4} (1×10^{-3}) m s^{-1} (*vdmin*)	5×10^{-3} (2×10^{-2}) m s^{-1} (*vdmax*)	
Wet deposition	5×10^{-5} h mm^{-1} s^{-1}	1×10^{-5} (*lmin*)	1×10^{-4} (*lmax*)	
Release height	Time varying (cf Table 1)	Diluted between 0 and 150 m (*Vertical_mixing*)		
Source term	Mathieu et al., 2012	Katata et al., 2012 (*Release_Chino*)	Stohl et al., 2011 (*Release_Stohl*)	Saunier et al., 2012 (*Release_Inverse*)
Rain	Rain radar observations	ECMWF forecasts (*ECMWF_rain*)		
Wind	ECMWF + observations at FNPP1	ECMWF forecasts (*ECMWF_wind*)		

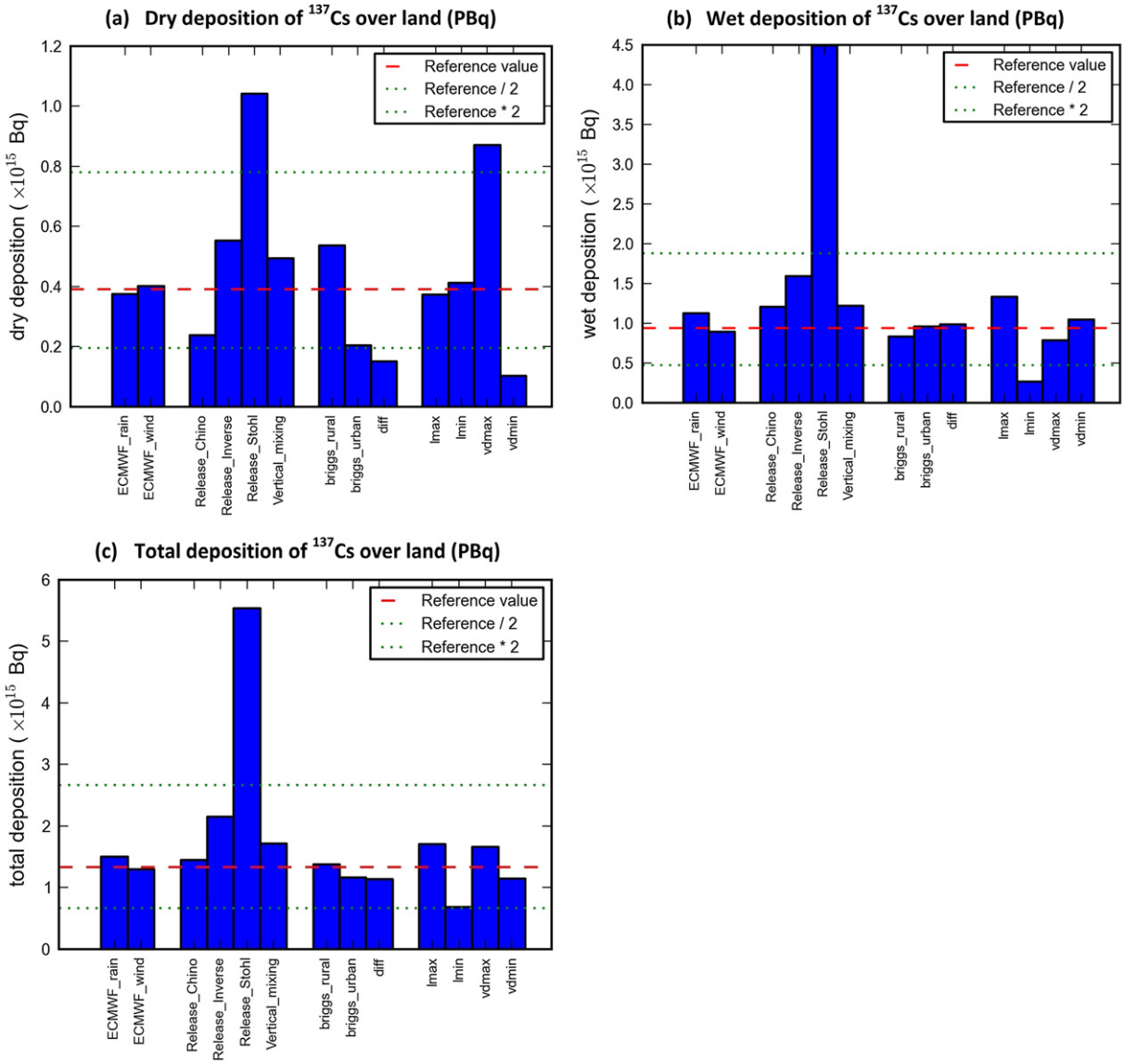

Fig. 9. Sensitivity of total ^{137}Cs deposition budget over land, within 80 km of FNPP1. Values for the reference simulation (similar to Table 3) are given in red (dashed lines). (For interpretation of the references to color in this figure legend, the reader is referred to the web version of this article.)

observations, would have 0.33 as FAC2 and 0.73 as FAC5, which is within the other simulations' results. Thus, other indicators such as FMS (Fig. 10(b)) and deposition maps (Supplementary material) are used as a complement.

The FMS is compared for a 10^5 Bq m^{-2} threshold which corresponds to the northwestern deposition. It is therefore sensitive to wet deposition parameters (*lmax*, *lmin*) and to the wind used during March 15th (*ECMWF_wind*). The *Release_Stohl* tends to overestimate deposition in the northwestern area, but is not penalized by this indicator, and the *Release_Chino* improves the FMS.

4.2.3. Sensitivity of gamma dose rates

Gamma dose rates are much more sensitive than deposition, which is integrated in time and has a better spatial coverage. With only eight stations, local discrepancies between model and reality on one station may have a huge impact on the results. Thus, a simulation may have acceptable results on deposition, but not on gamma dose rates. This is the case of *briggs_urban vertical_mixing* and *Release_inverse* simulations (Fig. 11). Lower dry deposition velocities improve the FMT by compensating for the overestimation due to errors in the source term and/or meteorological data. Dispersion parameters and source height have a much larger influence on gamma dose rates, especially peak values, than on deposition. This is particularly true on coastal stations, where the plume is very thin and the peak values are very sensitive to changes in the wind direction and diffusion. For instance, using a constant diffusion coefficient (*diff*) improves the results on coastal stations by increasing the plume vertical dilution in stable situations (Fig. 12(a) and (c)), thus reducing the overestimation. Using ECMWF forecasts without observations at FNPP1 (*ECMWF_wind*) drastically lowers the model performance on stations because of errors in the westerly wind direction on March 15th: Iitate and Fukushima are missed by the plume, and the peak at Koriyama is greatly overestimated (Fig. 12(b) and (d)). Fig. 12 illustrates the difficulty

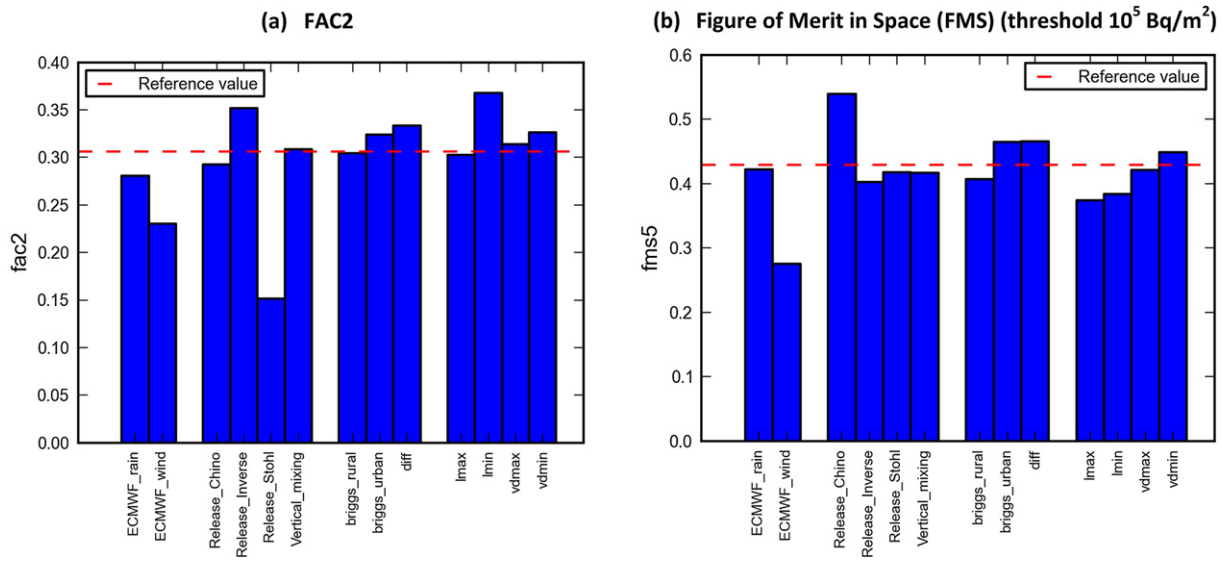

Fig. 10. Sensitivity of comparisons to MEXT measurements of ^{137}Cs, within 80 km of FNPP1. Values for the reference simulation are given in red (dashed line). (For interpretation of the references to color in this figure legend, the reader is referred to the web version of this article.)

to have a good model-to-data agreement (i.e. less than a factor 5) on all stations: the *Release_inverse* simulation greatly improves the results on coastal station but overestimates the northwestern peaks, while the *Release_chino* is better on northwestern stations but underestimates the peaks on southern and western stations.

5. Conclusions and perspectives

We presented atmospheric dispersion simulations of the Fukushima Nuclear Power Plant accident, using IRSN's Gaussian puff model pX. The evolution of atmospheric and ground activity simulated at local scale was presented with a "reference" simulation, whose performance was assessed through comparisons with environmental monitoring data (gamma dose rate and deposition). The results were within a factor of 2–5 of the observations for gamma dose rates, and 5–10 for deposition. The total quantity of ^{137}Cs deposed over land and the isotopic ratio ^{131}I/^{137}Cs were consistent with observations and with other estimations. The gamma dose rates in the northwestern area, highly contaminated by wet deposition, were correctly reproduced but the wet deposition zone was slightly misplaced. The coastal stations were more difficult to simulate, due to the stable situation inducing a thin plume, hence a large dependency to uncertainties in the wind direction and station location. Besides, the temporal frequency of measurements and/or wind fields may not be sufficient to correctly reproduce the peak values when the plume passed through the stations in less than 1 h. Thus, it is difficult to determine whether the overestimation along the coast is due to the source term, meteorological data and/or diffusion parameters.

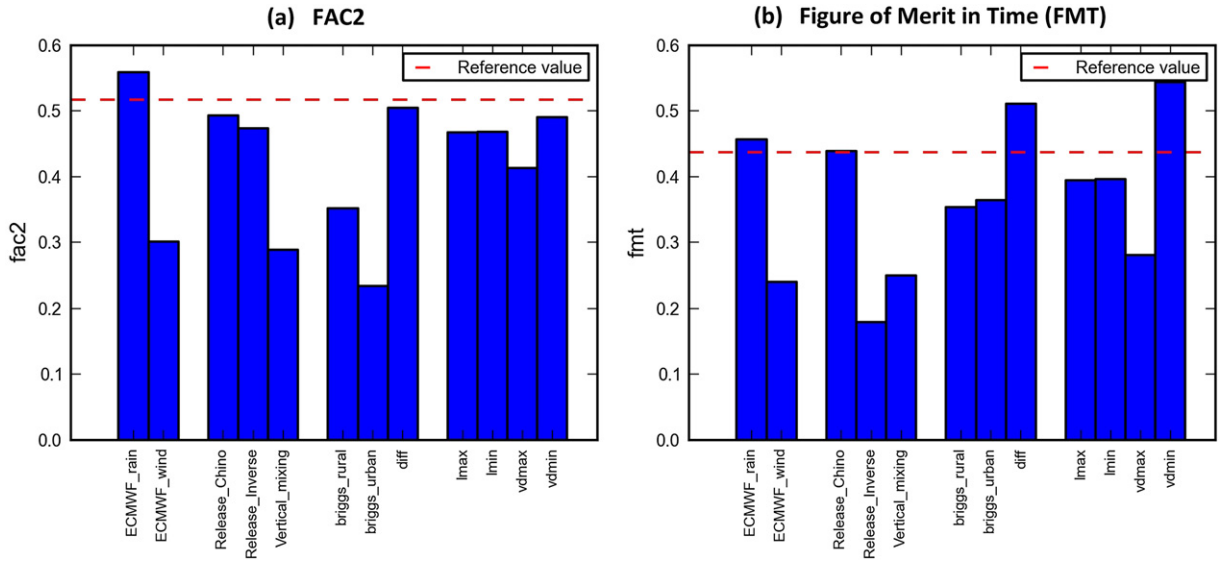

Fig. 11. Sensitivity of comparisons to gamma dose rate measurements on the eight monitoring stations. Values for the reference simulation are given in red (dashed line). (For interpretation of the references to color in this figure legend, the reader is referred to the web version of this article.)

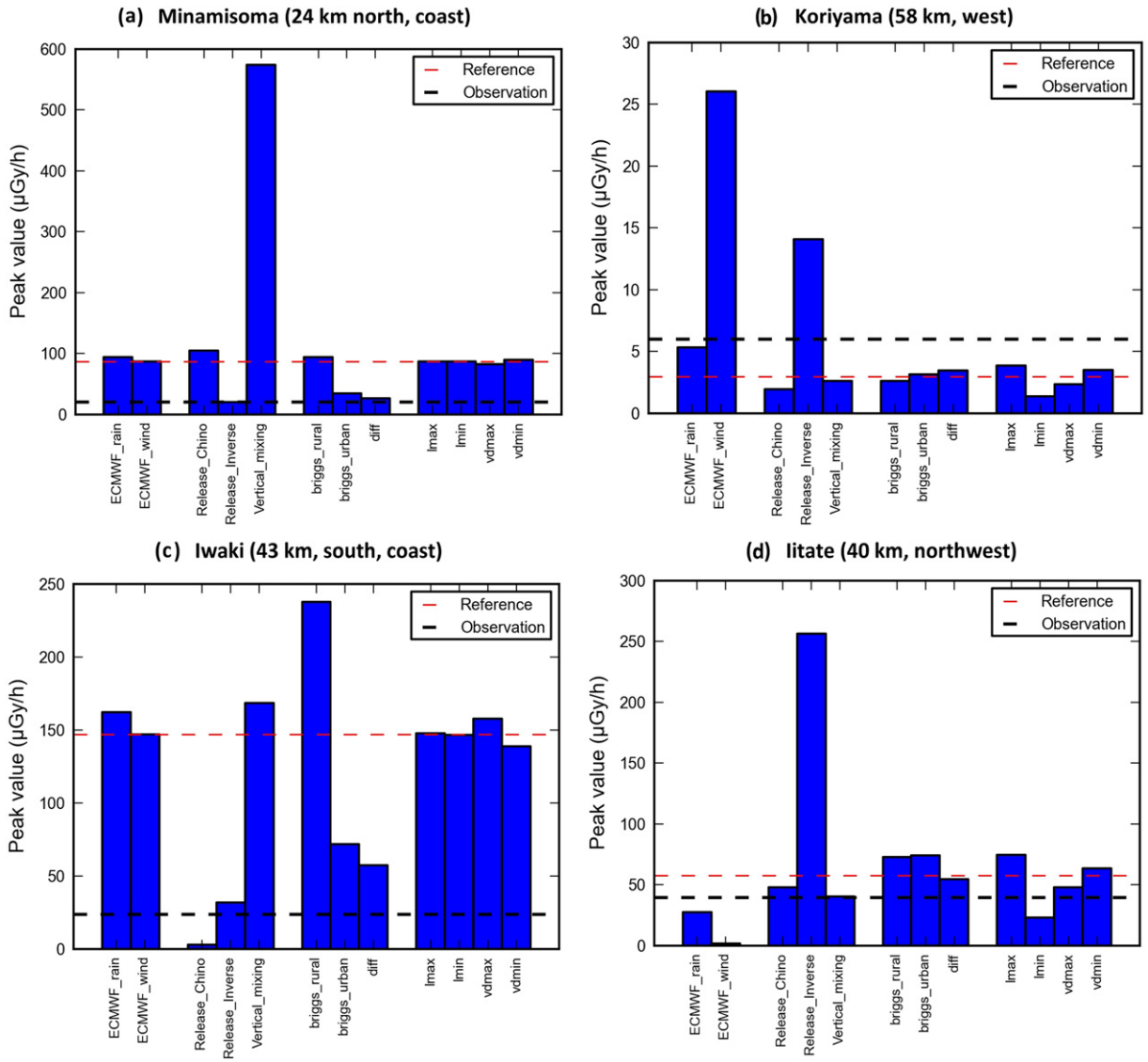

Fig. 12. Sensitivity of gamma dose rate peak values on four monitoring stations. Values for the reference simulation are given in red (dashed line). Observation values are given in black (bold dashed line). (For interpretation of the references to color in this figure legend, the reader is referred to the web version of this article.)

While uncertainties in the input data (wind direction, rain, source term kinetics and quantity) are huge, simulation parameters are also uncertain. The influence of each parameter was assessed separately. As expected, source terms had the highest impact on the results: the release from Stohl et al. (2011) tended to overestimation; that from Katata et al. (2012) gave better results on the northwest but underestimation in the south and west. Total deposition budget was within a factor 2 of the reference most of the time. The sensitivity study seemed to validate our choice for scavenging coefficients. Gamma dose rates, especially peak values, were quite sensitive: source terms, standard deviations, and wind direction had huge impacts on the results. However, with only eight monitoring stations, each station has a particular behavior and no general conclusions can be made.

This study is a first step toward updating model evaluation tools and proposing new indicators for modeling accidental releases of radionuclides. Despite the situation complexity and the remaining uncertainties, the results presented here are satisfactory compared to standard dispersion model evaluations. They can therefore be used as a benchmark for atmospheric dispersion models' evaluation and improvement with respect to emergency purposes. The main perspective is to use ensemble simulations instead of a single, deterministic model, in order to account for uncertainties in the input data and simulation parameters (Mallet and Sportisse, 2008). Another idea is to account for uncertainties in the plume position by comparing measurements to a cloud of points, or to an average over a given volume, instead of a single value.

Acknowledgments

We want to express our sympathy to Japanese people who endured the terrible consequences of the earthquake, tsunami and nuclear accident.

We thank MEXT and TEPCO for the online publication of measurements.

We thank Météo France for providing meteorological data, D. Corbin and J. Denis for the source term estimation, R. Gurriaran for

his expertise on measurements, and people from the Emergency Response Center who worked during the crisis.

Appendix A. Statistical indicators

We consider a set of measurements O_i (i between 1 and N) and the corresponding model outputs P_i. Statistical indicators are defined as follows (Chang and Hanna, 2004):

(1) Fractional bias MFBE:

$$\mathrm{MFBE} = \sum_{i=0}^{N} \frac{P_i - O_i}{P_i + O_i}$$

(2) Bias Factor at a given point:

$$\mathrm{BF} = \frac{P_i}{O_i}$$

(3) Correlation coefficient:

$$r = \frac{\sum_{i=1}^{N} \left(O_i - \overline{O}\right)\left(P_i - \overline{P}\right)}{\sqrt{\sum_{i=1}^{N} \left(O_i - \overline{O}\right)^2 \sum_{i=1}^{N} \left(P_i - \overline{P}\right)^2}}$$

(4) FAC2 (resp. FAC5): proportion of values such that $0.5 \leq \mathrm{BF} \leq 2$ (resp. $0.2 \leq \mathrm{BF} \leq 5$).

(5) The Figure of Merit in Time (FMT) is the percentage of overlap between measured and predicted integrated time series at a given location:

$$\mathrm{FMT} = \frac{\sum_{i=1}^{N} \min(O_i, P_i)}{\sum_{i=1}^{N} \max(O_i, P_i)}$$

(6) The Figure of Merit in Space (FMS) is the percentage of overlap between measured and predicted areas above a threshold T at a given time. A_P is the number of points verifying $P_i \geq T$ and A_O is the number of points such that $O_i \geq T$, then

$$\mathrm{FMS} = \frac{A_P \cap A_O}{A_P \cup A_O}$$

A “perfect” model-to-data agreement corresponds to MFBE = 0 and other indicators equal to 1.

Appendix B. Supplementary material

Supplementary material related to this article can be found at http://dx.doi.org/10.1016/j.atmosenv.2013.01.002.

References

Bailly du Bois, P., Laguionie, P., Boust, D., Korsakissok, I., Didier, D., 2012. Estimation of marine source-term following Fukushima Daiichi accident. Journal of Environmental Radioactivity 114, 2–9.

Baklanov, A., Sørensen, J.H., 2001. Parameterization of radionuclide deposition in atmospheric long-range transport modelling. Physics and Chemistry of the Earth (B) 26, 787–799.

Brandt, J., Christensen, J.H., Frohn, L., 2002. Modelling transport and deposition of caesium and iodine from the Chernobyl accident using the DREAM model. Atmospheric Chemistry and Physics 2, 397–417.

Chang, J.C., Hanna, S.R., 2004. Air quality model performance evaluation. Meteorology and Atmospheric Physics 87, 167–196.

Chino, M., Nakayama, H., Nagai, H., Terada, H., Katata, G., Yamazawa, H., 2011. Preliminary estimation of release amounts of ^{131}I and ^{137}Cs accidentally discharged from the Fukushima Daiichi Nuclear Power Plant into the atmosphere. Journal of Nuclear Science and Technology 48, 1129–1134.

Corbin, D., Denis, J., 2012. Evaluation des rejets atmosphériques liés à l'accident de Fukushima. IRSN. Report PSN-RES/SAG/2012–00347.

Eckerman, K.F., Ryman, J.C., 1993. Exposure-to-dose Coefficients for General Application, Based on the 1987 Federal Radiation Protection Guidance. Oak Ridge National Laboratory. Report 12.

IRSN, 2012. Fukushima, One Year Later: Initial Analyses of the Accident and Its Consequences. IRSN. Report IRSN/DG/2012-003. http://www.irsn.fr/EN/publications/technical-publications/Documents/IRSN_Fukushima-1-year-later_2012-003.pdf.

Katata, G., Ota, M., Terada, H., Chino, M., Nagai, H., 2012. Atmospheric discharge and dispersion of radionuclides during the Fukushima Daiichi Nuclear Power Plant accident. Part I: source term estimation and local-scale atmospheric dispersion in early phase of the accident. Journal of Environmental Radioactivity 109, 103–113.

Kinoshita, N., Sueki, K., Sasa, K., Kitagawa, J.-i., Ikarashi, S., Nishimura, T., Wong, Y.-S., Satou, Y., Handa, K., Takahashi, T., Sato, M., Yamagata, T., 2011. Assessment of individual radionuclide distributions from the Fukushima nuclear accident covering central-east Japan. Proceedings of the National Academy of Sciences 108 (49), 19526–19529.

Korsakissok, I., Mallet, V., 2009. Comparative study of Gaussian dispersion formulas within the Polyphemus platform: evaluation with Prairie Grass and Kincaid experiments. Journal of Applied Meteorology 48, 2459–2473.

Mallet, V., Sportisse, B., 2008. Air quality modeling: from deterministic to stochastic approaches. Computers & Mathematics with Applications 55, 2329–2337.

Mathieu, A., Korsakissok, I., Quélo, D., Groëll, J., Tombette, M., Didier, D., Quentric, E., Saunier, O., Benoit, J.-P., Isnard, O., 2012. Atmospheric dispersion and deposition of radionuclides from the Fukushima Daiichi nuclear power plant accident. Elements 8, 195–200.

Morino, Y., Ohara, T., Nishizawa, M., 2011. Atmospheric behavior, deposition, and budget of radioactive materials from the Fukushima Daiichi nuclear power plant in March 2011. Geophysical Research Letters 38, L00G11.

Pasquill, F.A., 1961. The estimation of the dispersion of windborne material. The Meteorological Magazine 90 (1063), 33–49.

Pryor, S.C., Barthelmie, R.J., Geernaert, L.L.S., Ellermann, T., Perry, K.D., 1999. Speciated particle dry deposition to the sea surface: results from ASEPS '97. Atmospheric Environment 33, 2045–2058.

Saunier, O., Mathieu, A., Didier, D., Tombette, M., Quélo, D., Winiarek, V., Bocquet, M., 2012. Using gamma dose rate monitoring with inverse modelling techniques to estimate the atmospheric release of a nuclear power plant accident: application to the Fukushima case. In: International Meeting on Severe Accident Assessment and Management: Lessons Learned from Fukushima Daiichi., San Diego, USA, 11–15 November 2012.

Soulhac, L., Didier, D., 2008. Projet pX, note de principe pX 1.0. IRSN. Report IRSN/DEI/SESUC/08-39.

Sportisse, B., 2007. A review of parameterization for modelling dry deposition and scavenging of radionuclides. Atmospheric Environment 41, 2683–2696.

Stohl, A., Seibert, P., Wotawa, G., Arnold, D., Burkhart, J.F., Eckhardt, S., Tapia, C., Vargas, A., Yasunari, T.J., 2011. Xenon-133 and caesium-137 releases into the atmosphere from the Fukushima Dai-ichi nuclear power plant: determination of the source term, atmospheric dispersion, and deposition. Atmospheric Chemistry and Physics Discussions 11, 28319–28394.

Terada, H., Katata, G., Chino, M., Nagai, H., 2012. Atmospheric discharge and dispersion of radionuclides during the Fukushima Dai-ichi Nuclear Power Plant accident. Part II: verification of the source term and analysis of regional-scale atmospheric dispersion. Journal of Environmental Radioactivity 112, 141–154.

Turner, D.B., 1969. Workbook of Atmospheric Dispersion Estimates.

Winiarek, V., Bocquet, M., Saunier, O., Mathieu, A., 2012. Estimation of errors in the inverse modeling of accidental release of atmospheric pollutant: application to the reconstruction of the cesium-137 and iodine-131 source terms from the Fukushima Daiichi power plant. Journal of Geophysical Research 117, D05122.